



Article

# Silver(I) Complexes Based on Oxadiazole-Functionalized $\alpha$ -Aminophosphonate: Synthesis, Structural Study, and Biological Activities

Shaima Hkiri <sup>1,2</sup>, Kübra Açıkalin Coşkun <sup>3</sup> , Elvan Üstün <sup>4</sup>, Ali Samarat <sup>2</sup>, Yusuf Tutar <sup>5</sup>, Neslihan Şahin <sup>6</sup> and David Sémeril <sup>1,\*</sup> 

- <sup>1</sup> Synthèse Organométallique et Catalyse, UMR-CNRS 7177, University of Strasbourg, 4 rue Blaise Pascal, 67008 Strasbourg, France
  - <sup>2</sup> Laboratory of Hetero-Organic Compounds and Nanostructured Materials (LR18ES11), Faculty of Sciences of Bizerte, University of Carthage, Bizerte 7021, Tunisia
  - <sup>3</sup> Department of Medical Biology and Genetics, Faculty of Medicine, University of İstanbul Aydın, İstanbul 34295, Turkey
  - <sup>4</sup> Department of Chemistry, Faculty of Art and Science, University of Ordu, Ordu 52200, Turkey
  - <sup>5</sup> Department of Basic Pharmaceutical Sciences, Faculty of Pharmacy, University of Health Sciences-Turkey, İstanbul 34668, Turkey
  - <sup>6</sup> Department of Science Education, Faculty of Education, University of Cumhuriyet, Sivas 58140, Turkey
- \* Correspondence: dsemeril@unistra.fr; Tel.: +33-(0)3-6885-1550



**Citation:** Hkiri, S.; Coşkun, K.A.; Üstün, E.; Samarat, A.; Tutar, Y.; Şahin, N.; Sémeril, D. Silver(I) Complexes Based on Oxadiazole-Functionalized  $\alpha$ -Aminophosphonate: Synthesis, Structural Study, and Biological Activities. *Molecules* **2022**, *27*, 8131. <https://doi.org/10.3390/molecules27238131>

Academic Editor: Yungen Liu

Received: 28 October 2022

Accepted: 16 November 2022

Published: 22 November 2022

**Publisher's Note:** MDPI stays neutral with regard to jurisdictional claims in published maps and institutional affiliations.



**Copyright:** © 2022 by the authors. Licensee MDPI, Basel, Switzerland. This article is an open access article distributed under the terms and conditions of the Creative Commons Attribution (CC BY) license (<https://creativecommons.org/licenses/by/4.0/>).

**Abstract:** Two silver(I) complexes, bis{diethyl[(5-phenyl-1,3,4-oxadiazol-2-yl- $\kappa N^3$ : $\kappa N^4$ -amino) (4-trifluoromethylphenyl)methyl]phosphonate-(tetrafluoroborate- $\kappa F$ )}-di-silver(I) and tetrakis-{diethyl[(5-phenyl-1,3,4-oxadiazol-2-yl- $\kappa N^3$ -amino)(4-trifluoromethylphenyl)methyl]phosphonate} silver(I) tetrafluoroborate, were prepared starting from the diethyl[(5-phenyl-1,3,4-oxadiazol-2-yl-amino)(4-trifluoromethylphenyl)methyl]phosphonate (1) ligand and  $AgBF_4$  salt in  $Ag$ /ligand ratios of 1/1 and 1/4, respectively. The structure, stoichiometry, and geometry of the silver complexes were fully characterized by elemental analyses, infrared, single-crystal X-ray diffraction studies, multinuclear NMR, and mass spectroscopies. The binuclear complex ( $[Ag_2(1)_2(BF_4)_2]$ ; **2**) crystallizes in the monoclinic asymmetric space group  $P2_1/c$  and contains two silver atoms adopting a  $\{AgN_2F\}$  planar trigonal geometry, which are simultaneously bridged by two oxadiazole rings of two ligands, while the mononuclear complex ( $[Ag(1)_4]BF_4$ ; **3**) crystallizes in the non-usual cubic space group  $Fd-3c$  in which the silver atom binds to four distinct electronically enriched nitrogen atoms of the oxadiazole ring, in a slightly distorted  $\{AgN_4\}$  tetrahedral geometry. The  $\alpha$ -aminophosphonate and the monomeric silver complex were evaluated in vitro against MCF-7 and PANC-1 cell lines. The silver complex is promising as a drug candidate for breast cancer and the pancreatic duct with half-maximal inhibitory concentration ( $IC_{50}$ ) values of  $8.3 \pm 1.0$  and  $14.4 \pm 0.6$   $\mu M$ , respectively. Additionally, the interactions of the ligand and the mononuclear complex with Vascular Endothelial Growth Factor Receptor-2 and DNA were evaluated by molecular docking methods.

**Keywords:** 1,3,4-oxadiazole; silver(I) complex; X-ray structure; in vitro cytotoxicity; MCF-7 cell line; PANC-1 cell line; molecular docking

## 1. Introduction

The coordination chemistry of silver(I), which displays a  $[Kr] 4d^{10} 5s^1$  electronic configuration, is particularly rich and can adopt a wide range of geometries [1–3]. In addition to linear silver(I) complexes [4–6], it is common to find triangular [7,8] or T-shaped [4,9], tetrahedral [10,11], or square plane [4,12] geometries but also compounds in which the silver atom is coordinated to five [13], six [13], seven [14], and even eight [15] ligands, often generating coordination polymers [16,17].

One of the most widely used coordinating atoms to silver has been found to be the nitrogen atom, which is generally incorporated in polydentate heterocyclic structures. Among these aza-heterocyclic ligands, 1,3,4-oxadiazoles have been well studied, leading to a wide coordination diversity of the silver cation [18–28]. For instance, Dong et al. reported the use of the 2,5-di(pyridin-4-yl)-1,3,4-oxadiazole ligand (**A**; Figure 1) with the  $\text{AgSO}_3\text{CF}_3$  metal precursor (metal/ligand ratio: 1/2) in a  $\text{CH}_2\text{Cl}_2/\text{MeOH}$  mixture, to obtain the infinite one-dimensional polymeric compound  $\{[\text{Ag}_4(\text{A})_4](\text{SO}_3\text{CF}_3)_4\}_n$  in a 71% yield. The single-crystal analysis revealed the presence of two different Ag(I) centers: the first one adopted nearly a linear coordination with the two pyridyl N-atoms from two **A** ligands, while the second one had a distorted trigonal coordination environment made of three N-donor atoms of two pyridyl and the 1,3,4-oxadiazole moieties. The tetramer formed a 40-membered macrocycle, which was further connected to a smaller 14-membered dimeric unit [29]. The same group reported the reaction of 2-(5-(2-hydroxyphenyl)-1,3,4-oxadiazol-2-yl)phenyl isonicotinate (**B**; Figure 1) with an equimolar amount of  $\text{AgPF}_6$ , which led to the formation of a bimetallic metallocycle of formula  $[\text{Ag}_2(\text{B})_2 \cdot (\text{MeOH})_2](\text{PF}_6)_2$  in which each Ag(I) center adopted a three-coordination sphere formed by one (N,O)-chelating donor and one pyridyl N-donor from a second **B** ligand. The two ligands arranged in a head-to-head fashion to form a distorted rectangular binuclear ring [30]. Recently, Qin et al. described the formation of a three-dimensional polymer from the 1,3,5-tris(5-(methylthio)-1,3,4-oxadiazol-2-yl)benzene ligand (**C**; Figure 1) and  $\text{AgSO}_3\text{CF}_3$  precursor (metal/ligand ratio: 3/1). The single crystal analysis revealed that the asymmetric unit is composed of two crystallographically independent silver cations, one ligand **C**, one coordinated water molecule, one coordinated triflate anion, a free counter anion, and a molecule of dichloromethane. The first Ag(I) adopts a distorted tetrahedral coordination sphere generated by four N(oxadiazole) atoms from four separate ligands. The second Ag(I) is also four-coordinated by two N(oxadiazole) atoms from two separate ligands and two oxygen atoms from a water molecule and a triflate anion. The polymeric network is generated by ligand **C**, which acts as a hexa-dentate ligand, binding to six Ag(I) cations. It is worth noting that, in the formed polymer, the sulfur atoms are not involved in the coordination with the metal [31]. An inorganic ribbon, formed by mixing (*E*)-3-(5-(furan-2-yl)-1,3,4-oxadiazol-2-yl)acrylic acid (**D**; Figure 1) and  $\text{AgNO}_3$  (metal/ligand ratio: 1/1) in the presence of a base, was reported by the group of Kokunov. In this polymer, two bidentate carboxylate groups bind two silver atoms and form dimeric blocks in which the Ag–Ag distance is only 2.854(1) Å. The distorted tetrahedral coordination of the Ag(I) cation is completed with an oxadiazole ring [32].

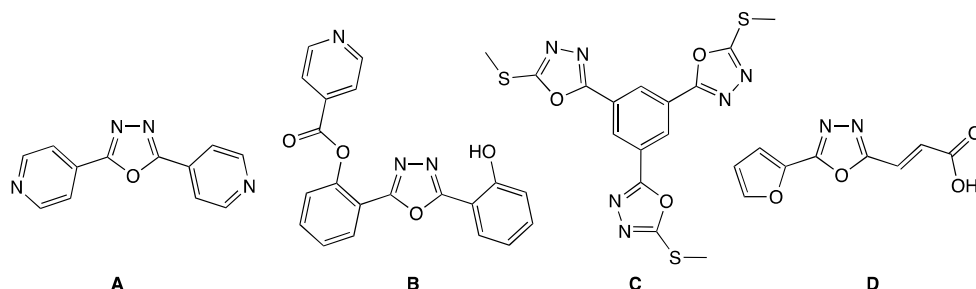


**Figure 1.** Examples of 1,3,4-oxadiazole-containing ligands **A–D** used in silver(I) complexes.

The possibility to modulate the coordination sphere of the silver(I) cation has allowed, in particular, the development of efficient silver complexes for medicinal applications, notably as antibacterial, antifungal, or anticancer agents [33–41]. In recent years, there has been growing interest in organic silver complexes as promising anticancer agents with efficacious activity against various cancer cell lines [42–44]. These complexes, which exhibit low toxicity for humans [45] and have long been used as antimicrobial drugs, are potential candidates to replace platinum-based anticancer drugs such as cisplatin (*cis*-diamminodichloroplatine(II)  $[\text{Pt}(\text{NH}_3)_2\text{Cl}_2]$ ) [46], which, despite their success, have drug

resistance, undesirable side-effects such as gastrointestinal disorders, bleeding, allergic reactions, or a decrease in immunity, and are effective against only a few types of cancer [47].

Angiogenesis is a physiological process of formation and development of new vessels from existing vessels [48]. The growth and spread of solid tumor cells require tumor angiogenesis [49]. There are many growth factors involved in tumor angiogenesis, one of the most notable of these is the vascular endothelial growth factor (VEGF) family [50]. The vascular endothelial growth factor receptors (VEGFRs) in mammalian cells include three members: VEGFR-1, VEGFR-2, and VEGFR-3 [51]. Among these three receptors, VEGFR-2 is considered to be the most important marker for endothelial cell development and directly regulates tumor angiogenesis [52]. Some studies reported that VEGFR-2 has been found in colon cancer, pancreatic cancer, small cell lung cancer, and breast cancer cells [53]. Therefore, managing the action mechanism of VEGFR-2 could be an effective way in the treatment of several types of cancer.

In this context, we now report the coordination of diethyl[(5-phenyl-1,3,4-oxadiazol-2-ylamino)(4-trifluoromethylphenyl)methyl]phosphonate to the silver cation  $\text{AgBF}_4$ . The cytotoxicities of the  $\alpha$ -aminophosphonate and one of its silver complexes were investigated toward the MCF-7 human breast cancer, which is the most frequently diagnosed cancer and the most common cause of death in women, and PANC-1 human pancreatic cancer cell lines. Our interest in this kind of ligand is stimulated by the well-known anticancer properties of 1,3,4-oxadiazoles [54] and  $\alpha$ -aminophosphonates [55–58], which could be beneficial for obtaining novel silver(I) complexes with enhanced anticancer activity. Additionally, the interactions of  $\alpha$ -aminophosphonate and one of its silver complexes against VEGFR-2 and DNA crystal structures were analyzed by molecular docking methods.

## 2. Results and Discussion

### 2.1. Silver(I) Complexes Synthesis

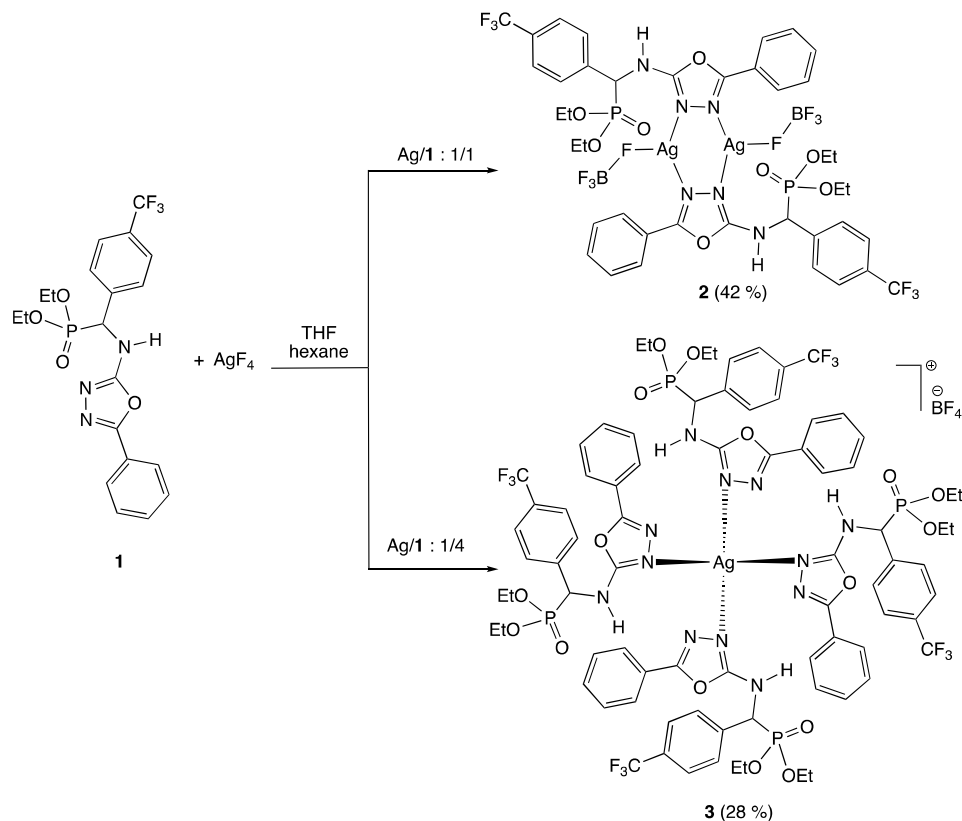
The slow diffusion of hexane into a THF solution of diethyl[(5-phenyl-1,3,4-oxadiazol-2-ylamino)(4-trifluoromethylphenyl)methyl]phosphonate (**1**) and  $\text{AgBF}_4$  led to crystals of silver- $\alpha$ -aminophosphonate adducts with various compositions and structures (Scheme 1). Infrared and mass spectrometry analysis carried out on the crystals revealed that the arrangement of the formed complexes depended exclusively on the metal-to-ligand ratio ( $\text{Ag}/\mathbf{1}$ ) used for the synthesis. Moreover, the IR spectrum of complex **2**, unlike complex **3**, displayed two weak bands at 724 and 751  $\text{cm}^{-1}$  and five broad bands in the range of 925–1067  $\text{cm}^{-1}$  consistent with a coordinated  $\text{BF}_4$  anion to a silver atom (see Supplementary Materials) [59].

Despite partial decomposition of complex **2** during the ESI-TOF analysis, cations with two silver atoms and a  $\text{BF}_4$  counter anion could be observed at  $m/z = 1666.18 [\text{M} + \mathbf{1} - \text{BF}_4]^+$  and 2121.30  $[\text{M} + (\mathbf{1})_2 - \text{BF}_4]^+$ . On the other hand, mass spectrum analysis of complex **3** displayed cations corresponding to  $m/z = 562.03 [\text{M} - (\mathbf{1})_3 - \text{BF}_4]^+$ , 1019.15  $[\text{M} - (\mathbf{1})_2 - \text{BF}_4]^+$ , 1474.27  $[\text{M} - \mathbf{1} - \text{BF}_4]^+$ , and 1929.40  $[\text{M} - \text{BF}_4]^+$  (Figure 2). Indeed, two different silver complexes, **2** ( $[\text{Ag}_2(\mathbf{1})_2(\text{BF}_4)_2]$ ) and **3** ( $[\text{Ag}(\mathbf{1})_4]\text{BF}_4$ ), were obtained starting from  $\text{Ag}/\mathbf{1}$  ratios of 1/1 and 1/4, in 42 and 28% yields, respectively (Scheme 1).

### 2.2. Single-Crystal X-ray Diffraction Studies

The binuclear complex **2** crystallized in the monoclinic asymmetric space group  $P2_1/c$  and contained two silver atoms, two distinct enantiomeric  $\alpha$ -aminophosphonate **1** (the two C9 atoms have an (*R*)- and an (*S*)-configuration), and two  $\text{BF}_4$  anions. The  $\text{CF}_3$  (F1, F2, and F3) moiety was disordered over two positions with a ratio of 0.6/0.4 (Figure 3 and Table 1). The silver atoms, which adopted  $\{\text{AgN}_2\text{F}\}$  planar trigonal geometries, were simultaneously bridged by two oxadiazole rings of two ligands with Ag1-N1 and Ag1-N2 bonds of 2.260(2) and 2.215(2) Å, respectively. The coordination spheres were completed with the coordination of the counter anion  $\text{BF}_4$  through a fluorine atom [23] (Ag-F4 2.652(2) Å; sum of van der Waals radii 3.27 Å [60]). The counter anion was also maintained by a hydrogen bond with the amine ( $\text{NH}_3 \cdots \text{F}_5$  2.117 Å). The distance between the two silver ions was 3.417 Å.

This distance was slightly smaller than the sum of the van der Waals radii of two silver ions (3.44 Å [60]), suggesting the occurrence of very weak argentophilic interactions [61]. The oxadiazole rings were planar with the phenyl substituents (dihedral angle of 3.03°) and angled with respect to the 4-trifluoromethylphenyl ring (dihedral angle of 44.21°).



**Scheme 1.** Synthesis of silver(I) complexes **2** and **3**.

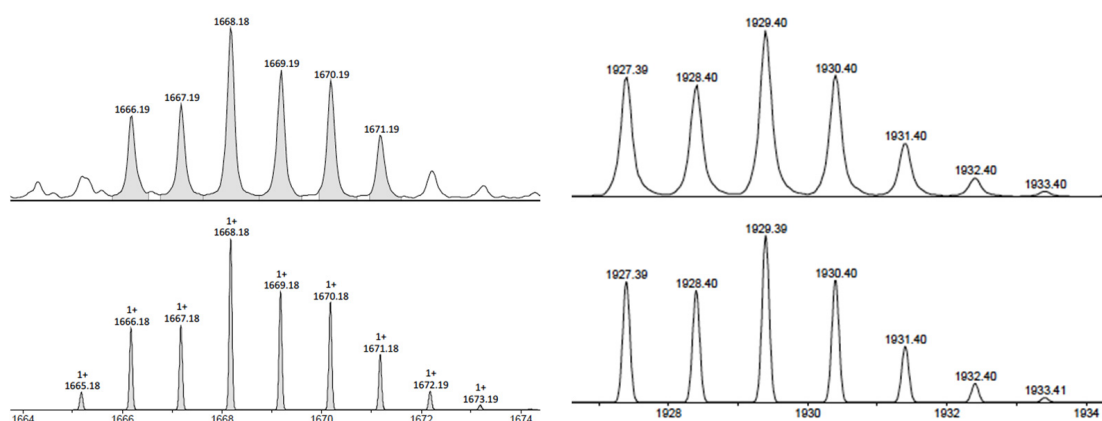


**Figure 2.** Mass spectrum (ESI-TOF) of silver complexes; observed spectrum (**Top**) and simulated spectrum (**Bottom**) for:  $(C_{20}H_{21}O_4N_3PF_3)_3Ag_2BF_4$  (**Left**) and  $(C_{20}H_{21}O_4N_3PF_3)_4Ag$  (**Right**).

The mononuclear complex **3** crystallized in the non-usual cubic space group *Fd-3c*. The silver atom bound to four distinct enantiomeric  $\alpha$ -aminophosphonates (the four C9 atoms had twice (*R*)- and twice (*S*)-configuration). The  $CF_3$  (F1, F2, and F3) and ethyl (C10 and C11) moieties were disordered over two positions with ratios of 0.5/0.5 and 0.57/0.43, respectively (Figure 4 and Table 1). The silver atoms adopted  $\{AgN_4\}$  slightly distorted tetrahedral geometries with Ag1-N1 bonds of 2.289(4) Å and N1-Ag1-N1 angles

of 105.56(10) or 117.6(2)°. The dihedral angles between the oxadiazole and the phenyl or the 4-trifluoromethylphenyl rings were 12.43 and 53.89°, respectively.

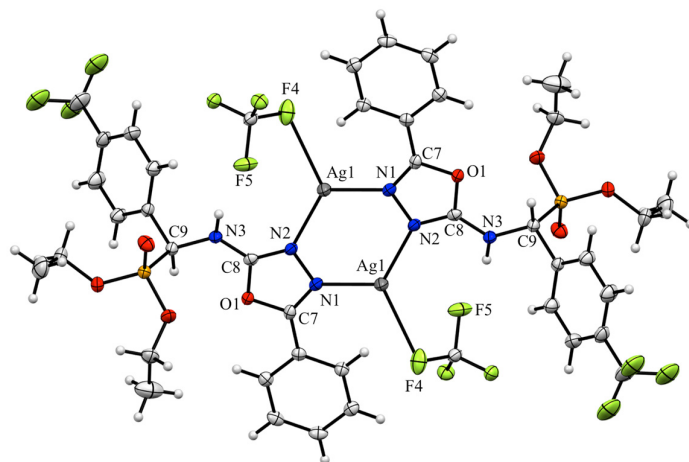


**Figure 3.** ORTEP drawing of complex **2**, 50% probability thermal ellipsoids. Important bond lengths (Å) and angles (°): Ag1–N1 2.260(2), Ag1–N2 2.215(2), Ag1–F4 2.652(2), N1–N2 1.406(3), N2–C8 1.311(4), C8–O1 1.353(3), O1–C7 1.372(3), C7–N1 1.293(4), N1–Ag1–F4 112.85(8), F4–Ag1–N2 123.02(7), N2–Ag1–N1 123.75(8), C7–N1–N2 107.4(2), N1–N2–C8 105.4(2), N2–C8–O1 112.3(2), C8–O1–C7 103.6(2), and O1–C7–N1 111.3(2).

**Table 1.** Crystal data and structure refinement parameters for complexes **2** and **3**.

Complex		2	3
CCDC Depository		2122361	2122362
Color/Shape		colorless/needle	colorless/prism
Chemical Formula		C <sub>40</sub> H <sub>42</sub> Ag <sub>2</sub> B <sub>2</sub> F <sub>14</sub> N <sub>6</sub> O <sub>8</sub> P <sub>2</sub>	C <sub>80</sub> H <sub>84</sub> AgBF <sub>16</sub> N <sub>12</sub> O <sub>16</sub> P <sub>4</sub>
Formula Weight (g mol <sup>−1</sup> )		1300.08	2016.15
Crystal System		monoclinic	cubic
Space Group		P2 <sub>1</sub> /c (number 14)	Fd-3c (number 228)
Unit Cell Parameters	a (Å)	21.2741 (8)	49.0604 (6)
	b (Å)	5.3745 (2)	49.0604 (6)
	c (Å)	21.0826 (9)	49.0604 (6)
	α (°)	90	90
	β (°)	96.259 (2)	90
	γ (°)	90	90
Volume (Å <sup>3</sup> )		2396.17 (16)	118,085 (4)
Z		2	48
D (g cm <sup>−3</sup> )		1.802	1.3361
μ (mm <sup>−1</sup> )		0.996	0.364
T <sub>min</sub> , T <sub>max</sub>		0.811, 0.907	0.951, 0.996
F(000)		1296	49,536
Crystal Size (mm)		0.220 × 0.120 × 0.100	0.140 × 0.120 × 0.012
Index Ranges		−27 ≤ h ≤ 27	−55 ≤ h ≤ 64
		−7 ≤ k ≤ 7	−64 ≤ k ≤ 41
		−27 ≤ l ≤ 27	−64 ≤ l ≤ 23
θ Range for Data Collection (°)		2.073 ≤ θ ≤ 27.907	2.034 ≤ θ ≤ 27.895
Reflections Collected		63,906	110,628
Independent/Observed		5699/4935	5899/3088
R <sub>int</sub>		0.0472	0.0762
Data/Restraints/Parameters		5699/0/337	5899/19/254
Goodness-of-Fit on F <sup>2</sup>		1.070	1.186
Final R Indices (I > 2.0 σ(I))		R <sub>1</sub> = 0.0371, wR <sub>2</sub> = 0.0823	R <sub>1</sub> = 0.0903, wR <sub>2</sub> = 0.2651
R Indices (All Data)		R <sub>1</sub> = 0.0458, wR <sub>2</sub> = 0.880	R <sub>1</sub> = 0.1435, wR <sub>2</sub> = 0.3072
Δρ <sub>max</sub> , Δρ <sub>min</sub> (e Å <sup>−3</sup> )		1.471, −1.066	0.689, −0.553



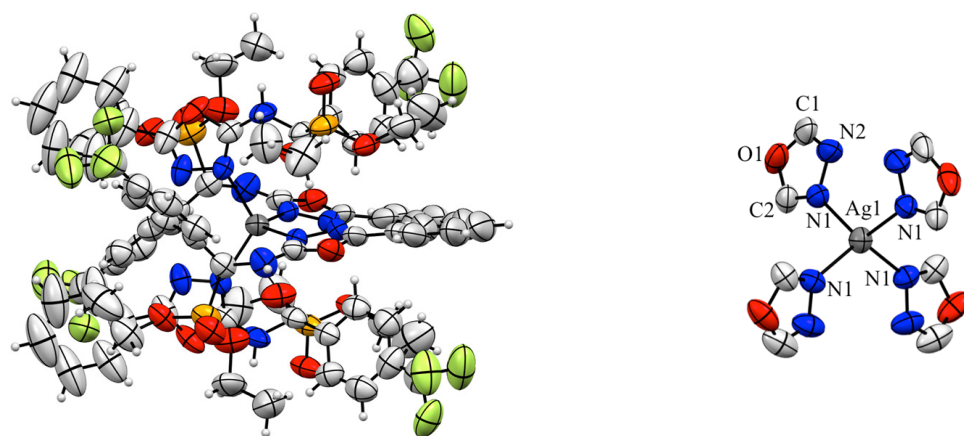


**Figure 4.** ORTEP drawing of complex **3**, 50% probability thermal ellipsoids ( $\text{BF}_4$  and solvent molecules are not visible). Important bond lengths ( $\text{\AA}$ ) and angles ( $^\circ$ ): Ag1-N1 2.289(4), Ag1-N1 2.289(4), Ag1-N1 2.289(4), Ag1-N1 2.289(4), N1-N2 1.412(6), N2-C1 1.250(9), C1-O1 1.356(9), O1-C2 1.372(7), C2-N1 1.283(7), N1-Ag1-N1 105.56(10), N1-Ag1-N1 117.6(2), N1-Ag1-N1 105.56(10), N1-Ag1-N1 105.56(10), N1-Ag1-N1 117.6(2), N1-Ag1-N1 105.56(10), C2-N1-N2 105.7(5), N1-N2-C1 107.3(6), N2-C1-O1 112.7(6), C1-O1-C2 102.8(5), and O1-C2-N1 111.5(5).

The study revealed the presence in the solid state, for each silver complex, of eight hydrogen bonds involving their N-H and P=O moieties [62] ( $\text{H}\cdots\text{O}$  1.877  $\text{\AA}$ ) supramolecularly interlinked to each complex with four neighbors around the three crystallographic axes. In the crystal lattice (118,085(4)  $\text{\AA}^3$ ), the 48  $[\text{Ag}(1)_4]$  cations generated a three-dimensional microporous supramolecular network, which contained a void between the inorganic molecules (18,208  $\text{\AA}^3$ ). At the end of the crystal structure determination, residual electron density peaks (4825 e $^-$ ) were found for which no satisfactory disorder model could be obtained. The disordered species were a mixture of counter anion  $\text{BF}_4$  (1968 e $^-$ ) and solvent molecules (2857 e $^-$ ), occupying the space left vacant by the silver complexes [31]. The SQUEEZE program was used to account for the disorder. The contribution of these species was removed from the final structure factor calculations (see Supplementary Materials).

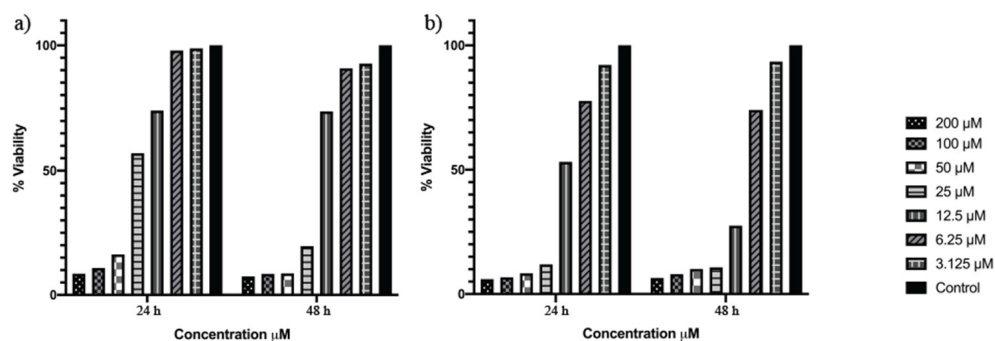
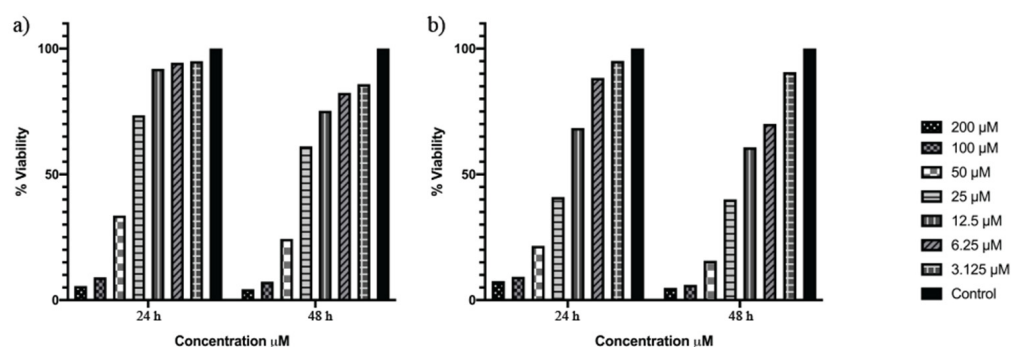
It is interesting to note that in both silver complexes, the potentially coordinating group  $\text{P}(\text{O})(\text{OEt})_2$  was not involved in a coordination with the metal centers.

### 2.3. In Vitro Effects Assessment on MCF-7 and PANC-1 Cell Lines

Preliminary in vivo toxicity studies carried out on brain of mice demonstrated that the monomeric silver complex **3** is not neurotoxic contrary to the dimeric complex **2** [63]. Consequently, the antitumor potential of the  $\alpha$ -aminophosphonate **1** and the tetrahedral silver complex **3** were evaluated against MCF-7 and PANC-1 cells by a one-dose assay. The 3-(4,5-dimethylthiazol-2-yl)-2,5-diphenyl tetrazolium bromide (MTT) assays were performed to investigate the dose-dependent silver compounds' effect on cell viability. For this purpose, compounds were added on cells at an increasing concentration (3.125–200  $\mu\text{M}$ ) during 24 and 48 h and  $\text{IC}_{50}$  values were calculated (Table 2). After 24 h of incubation, the results indicated that  $\alpha$ -aminophosphonate **1** was about twice less cytotoxic than the silver complex **3**, and  $\text{IC}_{50}$  values of  $22.8 \pm 0.8$  and  $11.2 \pm 0.4$   $\mu\text{M}$  were obtained when the MCF-7 cell line was treated with **1** and **3**, respectively (Figure 5). Both compounds had a dose-dependent effect and, when exposed to the PANC-1 cell line, they showed lower cytotoxicity with  $\text{IC}_{50}$  values of  $35.0 \pm 1.0$  and  $18.3 \pm 1.2$   $\mu\text{M}$  for **1** and **3**, respectively (Figure 6).

**Table 2.** Calculated IC<sub>50</sub> values (μM).

Tested Compound	24 h		48 h	
	MCF-7 Cell Line	PANC-1 Cell Line	MCF-7 Cell Line	PANC-1 Cell Line
<b>1</b>	22.8 ± 0.8	35.0 ± 1.0	14.9 ± 0.5	27.6 ± 0.7
<b>3</b>	11.2 ± 0.4	18.3 ± 1.2	8.3 ± 1.0	14.4 ± 0.6

**Figure 5.** MCF-7 cells were treated with increasing concentrations of  $\alpha$ -aminophosphonate **1** (a) and silver complex **3** (b) for 24 and 48 h. The viability was determined by metabolic rate using the MTT assay. Absorbance values were measured at 570 nm and normalized against untreated cells.**Figure 6.** PANC-1 cells were treated with increasing concentrations of  $\alpha$ -aminophosphonate **1** (a) and silver complex **3** (b) for 24 and 48 h. The viability was determined by metabolic rate using the MTT assay. Absorbance values were measured at 570 nm and normalized against untreated cells.

The two drugs **1** and **3** had a time-dependent effect; the cytotoxicities could be improved by extending the incubation time to 48 h. Thus, with the silver complex **3**, IC<sub>50</sub> values of  $8.3 \pm 1.0$  and  $14.4 \pm 0.6$  μM were observed on MCF-7 and PANC-1 cell lines, respectively. The IC<sub>50</sub> values are slightly higher than those previously reported in the literature for cisplatin,  $5.7 \pm 0.1$  (incubation for 24 h) and  $14.4 \pm 1.1$  (incubation for 48 h) for MCF-7 [64] and PANC-1 [65] cell lines, respectively.

Comparison with other organometallic silver complexes tested on MCF-7 and PANC-1 cell lines, such as silver(I) complexes in which the metal is coordinated to carbon [6,66], phosphorus [67,68], or nitrogen [69] atoms, showed that  $\alpha$ -aminophosphonate **1** and complex **3** exhibited comparable effects (Figure 7).

#### 2.4. Molecular Docking Studies

Molecular docking is a frequently used method in detailed bioactivity analysis of molecules [70]. It is possible to make qualitative and quantitative evaluations of the interactions between target macromolecule crystals and candidate bioactive molecules [71]. While the interaction areas qualitatively indicate how the ligand and the biological macromolecule will interact, the relative value of the binding can be considered as a quantitative measurement of the affinity. High ligand binding affinity means both stronger interaction

between the ligand and target molecule and measurement of the ligand concentration required for inhibition [72].

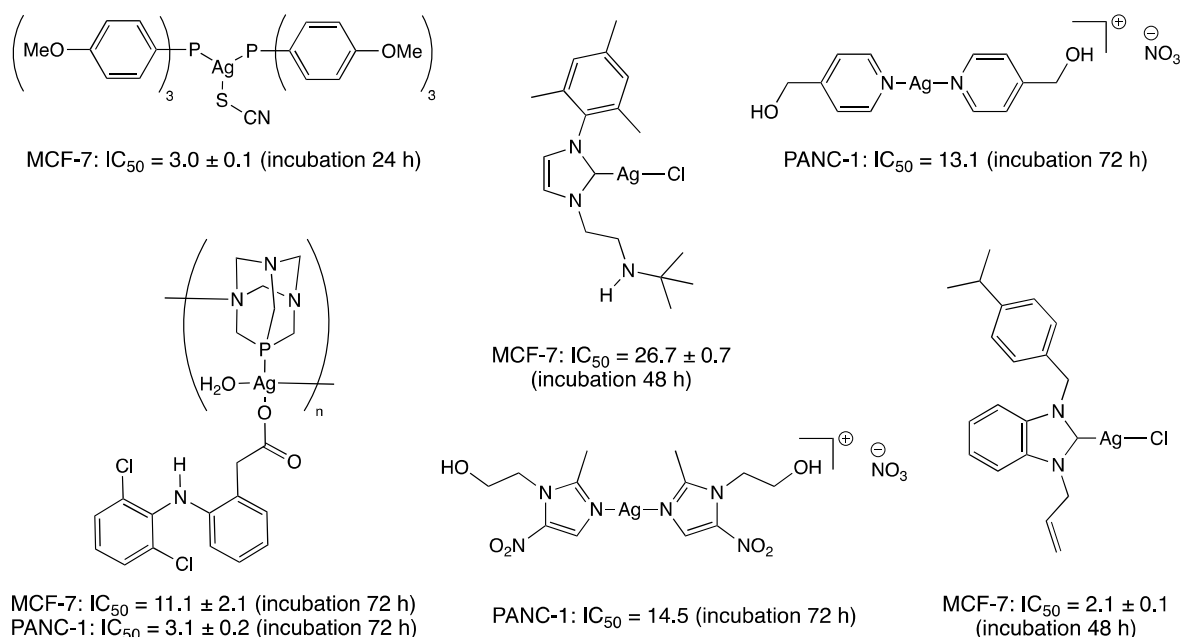


**Figure 7.** Examples of reported silver(I) complexes with anticancer activities.

Boda et al. synthesized some new isatin-1,2,4-oxadiazole derivative molecules and analyzed the activity of these molecules against some cancer cell lines including MCF-7. The authors analyzed the interactions between these molecules and the VEGFR-2 crystal structure and recorded a binding energy of  $-10.85$  kcal/mol [73]. Serdaroğlu et al. reported the in vitro cytotoxic activities of silver complexes coordinated to *N*-heterocyclic carbene ligands. The study showed that the organometallic molecules could be efficient anti-cancer agents with a binding affinity of  $-7.59$  kcal/mol [74]. Although there are many studies of molecular docking, which analyzed the anticancer activities of aminophosphonate derivatives and their metal complexes, a finite number of them have focused on the interactions with VEGFR-2 for a detailed analysis of anticancer activity [75–79].

In our work, the  $\alpha$ -aminophosphonate **1** was optimized with the ORCA package program [80,81] and the most stable structure interacted with the VEGFR-2 crystal structure [82]. Some interactions for the ligand were detected: (i) four H-bonds between the ligand and Asp1044, Cys1043, Glu883, and Lys866 with lengths of 2.19, 3.66, 2.91, and 3.00 Å, respectively; (ii)  $\pi$ -alkyl interactions with Ala864, Val897, Val914, Cys917, and Leu1033; (iii) van der Waals interactions; (iv) halogenic interaction of the  $CF_3$  with Arg 1030. The total energy of all these interactions was  $-7.58$  kcal/mol. The binding sites of the ligand and the silver complex **3** were different due to the larger steric hindrance of the complex. Complex **3** carried out fewer interactions but they were stronger than **1**, and the most important interactions were H-bonds with Asp1044, Arg1078, and Arg1025 with lengths of 2.75, 3.20, and 3.07 Å, respectively. Additional van der Waals and alkyl interactions contributed to the total binding between the silver complex and the target molecule. The total value of these interactions was calculated at  $-7.82$  kcal/mol (Figure 8). The results show that the silver complex **3** will bind more effectively than the  $\alpha$ -aminophosphonate **1**, and will, therefore, be a more effective inhibitor. These results are also in agreement with the experimental anticancer results *vide supra*.



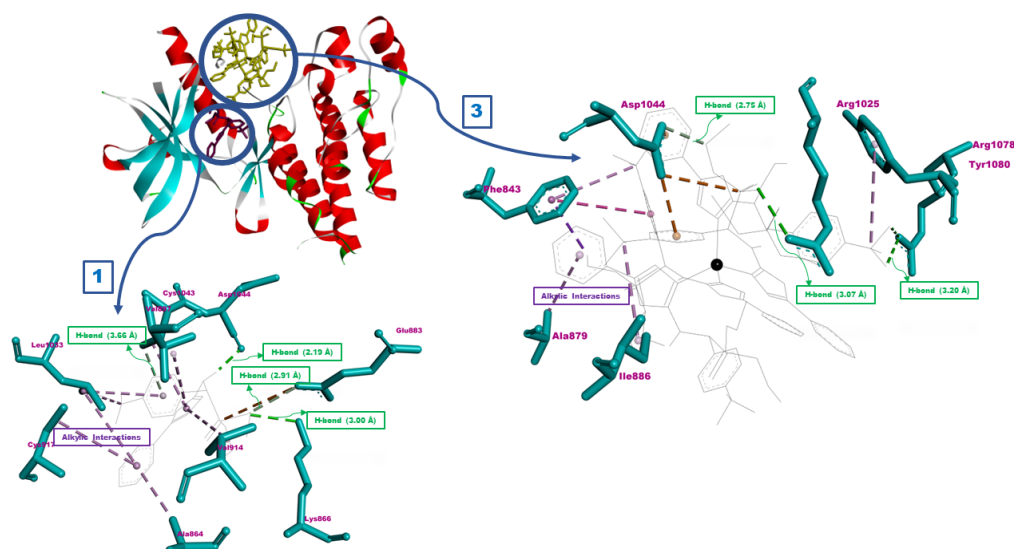


**Figure 8.** Interaction residue and interaction type of the molecules (1 and 3) with VEGFR-2 crystal structure.

Molecular docking is also a frequently used method for analyzing the interaction of molecular pharmaceuticals with DNA [83]. The B-DNA dodecamer (1bna) crystal structure was used to determine the interaction modes of molecules with DNA [84]. Both molecules (1 and 3) interact with approximately the same regions of DNA. While the  $\alpha$ -aminophosphonate 1 interacted with the region consisting of Thy8, Cyt9, Gua10, Cyt11, and Gua12, the silver complex 3 additionally interacted with Ade6 and Thy7. The final interaction energies were determined as  $-6.9$  and  $-7.86$  kcal/mol for 1 and 3, respectively (Figure 9).

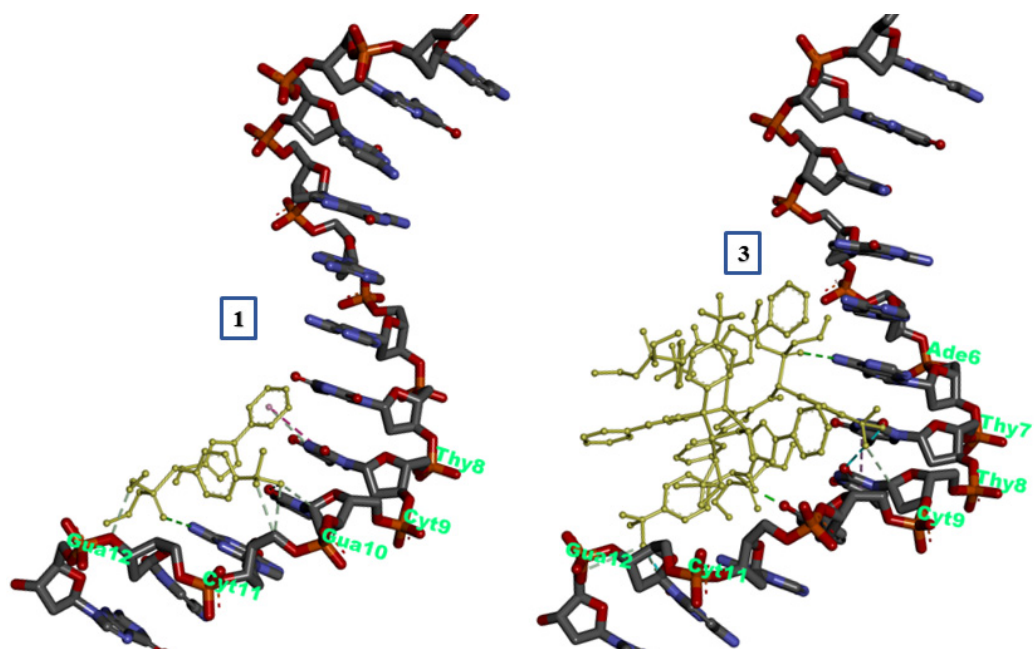


**Figure 9.** Interaction residue and amino acids of DNA crystal structures with 1 and 3.

### 3. Materials and Methods

All manipulations were carried out under dry argon. Solvents were dried by conventional methods and were distilled immediately before use. Routine  $^1\text{H}$ ,  $^{31}\text{P}\{^1\text{H}\}$ , and  $^{19}\text{F}\{^1\text{H}\}$  spectra were recorded with Bruker FT instruments (AC 300 and 500).  $^1\text{H}$  NMR spectra were referenced to residual protonated solvents ( $\delta = 7.26$  ppm for  $\text{CDCl}_3$ ).  $^{31}\text{P}$  and  $^{19}\text{F}$  NMR spectroscopic data are given relative to external  $\text{H}_3\text{PO}_4$  and  $\text{CCl}_3\text{F}$ , respectively. Chemical shifts and coupling constants are reported in ppm and Hz, respectively. Infrared spectra were recorded with a Bruker FT-IR Alpha-P spectrometer. The optical density was measured at 570 nm with an ELISA Microplate Reader spectrophotometer. Elemental analyses were carried out by the Service de Microanalyse, Institut de Chimie, Université de Strasbourg. Diethyl[(5-phenyl-1,3,4-oxadiazol-2-ylamino)(4-trifluoromethylphenyl)methyl]phosphonate (**1**) was prepared by a literature procedure [85].

#### 3.1. General Procedure for the Synthesis of the Silver(I) Complexes

A solution of  $\text{Ag}(\text{BF}_4)$  (0.019 g, 0.10 mmol) in THF (2 mL) was added to a solution of diethyl[(5-phenyl-1,3,4-oxadiazol-2-ylamino)(4-trifluoromethylphenyl)methyl]phosphonate (**1**, 0.10 or 0.4 mmol for the synthesis of **2** and **3**, respectively) in THF (10 mL). The reaction mixture was stirred in the dark for 16 h at room temperature. The solvent was removed under reduced pressure. Crystals were grown from a slow diffusion of hexane into a solution of the crude product, dissolved into the minimal amount of THF. The colorless crystals of the silver complex were collected and dried under vacuum.

##### 3.1.1. Bis{diethyl[(5-phenyl-1,3,4-oxadiazol-2-yl- $\kappa\text{N}^3$ : $\kappa\text{N}^4$ -amino)(4-trifluoromethylphenyl)methyl]phosphonate-(tetrafluoroborate- $\kappa\text{F}$ )}-di-silver(I) (**2**)

Yield 42%.  $^1\text{H}$  NMR (300 MHz,  $\text{CDCl}_3$ ):  $\delta = 7.85$  (dd, 4H, arom. CH of  $\text{CF}_3\text{C}_6\text{H}_4$ ,  $^3J_{\text{HH}} = 6.9$  Hz,  $^4J_{\text{HH}} = 1.8$  Hz), 7.71–7.62 (m, 8H, arom. CH), 7.49–7.42 (m, 6H, arom. CH), 5.28 (d, 2H, CHP,  $^2J_{\text{PH}} = 22.5$  Hz), 4.24–4.11 (m, 4H,  $\text{OCH}_2\text{CH}_3$ ), 4.03–3.81 (m, 4H,  $\text{OCH}_2\text{CH}_3$ ), 1.32 (t, 6H,  $\text{OCH}_2\text{CH}_3$ ,  $^3J_{\text{HH}} = 7.2$  Hz), 1.15 (t, 6H,  $\text{OCH}_2\text{CH}_3$ ,  $^3J_{\text{HH}} = 7.1$  Hz) ppm, in the spectrum, the two NH protons are not observed;  $^{31}\text{P}\{^1\text{H}\}$  NMR (121 MHz,  $\text{CDCl}_3$ ):  $\delta = 19.1$  (q, P(O),  $^7J_{\text{PF}} = 2.0$  Hz) ppm.  $^{19}\text{F}\{^1\text{H}\}$  NMR (282 MHz,  $\text{CDCl}_3$ ):  $\delta = -62.72$  (d,  $\text{CF}_3$ ,  $^7J_{\text{PF}} = 2.2$  Hz),  $-147.92$  (brs,  $\text{BF}_4$ ) ppm. IR:  $\nu = 724, 751, 925, 954, 1017, 1031, 1067$  ( $\text{F}_3\text{BF-Ag}$ ),  $1658\text{ cm}^{-1}$  (C=N). MS (ESI-TOF): decomposition of the complex occurred during the analysis, although some cations containing two silver complex could be observed at  $m/z = 1666.18$  [ $\text{M} + \mathbf{1} - \text{BF}_4$ ] $^+$  and  $2121.30$  [ $\text{M} + (\mathbf{1})_2 - \text{BF}_4$ ] $^+$  (expected isotopic profile). Elemental analysis calcd. (%) for  $\text{C}_{40}\text{H}_{42}\text{Ag}_2\text{B}_2\text{F}_{14}\text{N}_6\text{O}_8\text{P}_2$  (1300.08): C 36.95, H 3.26, N 6.46; found C 35.85, H 3.14, N 6.27.

##### 3.1.2. Tetrakis-{diethyl[(5-phenyl-1,3,4-oxadiazol-2-yl- $\kappa\text{N}^3$ -amino)(4-trifluoromethylphenyl)methyl]phosphonate}silver(I) Tetrafluoroborate (**3**)

Yield 28%.  $^1\text{H}$  NMR (300 MHz,  $\text{CDCl}_3$ ):  $\delta = 7.86$  (dd, 8H, arom. CH of  $\text{CF}_3\text{C}_6\text{H}_4$ ,  $^3J_{\text{HH}} = 7.8$  Hz,  $^4J_{\text{HH}} = 1.2$  Hz), 7.74–7.62 (m, 16H, arom. CH), 7.54–7.44 (m, 12H, arom. CH), 5.34 (d, 4H, CHP,  $^2J_{\text{PH}} = 21.9$  Hz), 4.24–4.14 (m, 8H,  $\text{OCH}_2\text{CH}_3$ ), 4.08–3.90 (m, 8H,  $\text{OCH}_2\text{CH}_3$ ), 1.32 (t, 12H,  $\text{OCH}_2\text{CH}_3$ ,  $^3J_{\text{HH}} = 7.0$  Hz), 1.20 (t, 12H,  $\text{OCH}_2\text{CH}_3$ ,  $^3J_{\text{HH}} = 7.0$  Hz) ppm; in the spectrum, the four NH protons are not observed;  $^{31}\text{P}\{^1\text{H}\}$  NMR (121 MHz,  $\text{CDCl}_3$ ):  $\delta = 17.9$  (q, P(O),  $^7J_{\text{PF}} = 2.2$  Hz) ppm.  $^{19}\text{F}\{^1\text{H}\}$  NMR (282 MHz,  $\text{CDCl}_3$ ):  $\delta = -62.77$  (d,  $\text{CF}_3$ ,  $^7J_{\text{PF}} = 2.2$  Hz),  $-148.47$  (s,  $\text{BF}_4$ ) ppm. IR:  $\nu = 1633\text{ cm}^{-1}$  (C=N). MS (ESI-TOF):  $m/z = 562.03$  [ $\text{M} - (\mathbf{1})_3 - \text{BF}_4$ ] $^+$ ,  $1019.15$  [ $\text{M} - (\mathbf{1})_2 - \text{BF}_4$ ] $^+$ ,  $1474.27$  [ $\text{M} - \mathbf{1} - \text{BF}_4$ ] $^+$  and  $1929.40$  [ $\text{M} - \text{BF}_4$ ] $^+$  (expected isotopic profile). Elemental analysis calcd. (%) for  $\text{C}_{80}\text{H}_{84}\text{AgBF}_{16}\text{N}_{12}\text{O}_{16}\text{P}_4$  (2016.14): C 47.66, H 4.20, N 8.34; found C 47.54, H 4.33, N 8.21.

#### 3.2. X-Crystal Structure Analysis

Single crystals suitable for X-ray analysis were obtained by the slow diffusion of hexane into a THF solution of the complex. The samples were studied on a Bruker PHOTON-III CPAD and Bruker APEX-II CD for complexes **2** and **3**, respectively, using  $\text{Mo-K}_\alpha$  radiation

( $\lambda = 0.71073 \text{ \AA}$ ) at  $T = 120(2) \text{ K}$ . The structures were solved with SHELXT-2014/5 [86] (complex 2) or SHELXS-97 [87] (complex 3), which revealed the non-hydrogen atoms of the molecule. After anisotropic refinement, all of the hydrogen atoms were found with a Fourier difference map. The structure was refined with SHELXL-2014/7 [88] by the full-matrix least-square techniques (use of  $F$  square magnitude;  $x, y, z, \beta_{ij}$  for C, Ag, B, F, N, O, and P atoms;  $x, y, z$  in riding mode for H atoms).

### 3.3. Cell Culture and Cell Viability Assay

The experiments were performed on MCF-7 (human breast cancer, HTB-22) and PANC-1 (human pancreatic cancer, CRL-1469) cell lines. The cell lines obtained from the American Type Culture Collection and were cultivated on 10% fetal bovine serum (FBS), 1% L-glutamine, and 100 IU/mL of penicillin and 10 mg/mL of streptomycin containing high-glucose Dulbecco's modified Eagle's medium (DMEM) (Gibco™, Sigma). Cells were cultivated in a humidified atmosphere with 5%  $\text{CO}_2$  at  $37^\circ\text{C}$ .

The cytotoxic activity of compound 1 and silver complex 3 on cells was evaluated using the 3-(4,5-dimethylthiazol-2-yl)-2,5-diphenyl tetrazolium bromide (MTT) method as previously described by Mosmann [89] with slight modifications. Cells (7000 per 200  $\mu\text{L}$ ) in medium were seeded into 96-well microplates. Compound 1 or 3 was added to the wells by serial dilution (200  $\mu\text{M}$ , 100  $\mu\text{M}$ , 50  $\mu\text{M}$ , 25  $\mu\text{M}$ , 12.5  $\mu\text{M}$ , 6.25  $\mu\text{M}$ , and 3.125  $\mu\text{M}$ ) and the cells were incubated at  $37^\circ\text{C}$  in a 5%  $\text{CO}_2$  incubator for 24 h and 48 h. At the end of the incubation time, the MTT reagent (20  $\mu\text{L}$ ) was added and the cells were incubated for a further 4 h. The formed formazan crystals were dissolved in 100  $\mu\text{L}$  of DMSO and the absorptions were measured at 570 nm with an ELISA Microplate Reader. Experiments were performed five times and the  $\text{IC}_{50}$  values, which corresponds to the concentration required for 50% inhibition of cell viability, were calculated by Graphpad prism software (version 8.2.1, San Diego, CA, USA). Results were expressed as percentage of viable cells relative to the negative control (untreated cells).

### 3.4. Molecular Docking Calculation Methods

The molecular docking procedures were performed with AutoDock 4.2 [90] against VEGFR-2 and B-DNA dodecamer crystal structures [82,84]. All the structures were downloaded from the RCSB protein data bank (<https://www.rcsb.org/>, accessed on 20 October 2022) (PDB ID: 1ywn for VEGFR-2; 1bna for B-DNA dodecamer, accessed on 16 August 2022). The maximum torsion number with the fewest atoms was set for the ligand molecules. Kollman charges were regarded, and only polar hydrogens were employed in all target crystal structures. Water molecules in the targets were extracted as well as Gasteiger charges, and randomized starting positions were utilized during the processes. Lamarckian genetic algorithms were employed with 150 genetic algorithm populations for 10 runs [91]. The standard program defaults were used during the running. All the illustrations were performed with Discovery Studio 4.1.0. (BIOVIA Corp, San Diego, CA, USA).

## 4. Conclusions

A simple modification of the silver salt to ligand, bearing an oxadiazole ring, to silver salt ratio drastically modified the coordination sphere of silver(I) cations, leading either to a trigonal dimeric or to a tetrahedral monomeric silver complex. The  $\alpha$ -aminophosphonate and the monomeric silver complex were evaluated in vitro against MCF-7 and PANC-1 cell lines by a one-dose assay. The presence of a silver atom had a beneficial effect on the cytotoxic activities, and approximately twofold lower half-maximal inhibitory concentration ( $\text{IC}_{50}$ ) values were observed when the organometallic complex was employed compared to the organic drug. The silver complex is promising as a drug candidate for breast cancer and the pancreatic duct and future studies will be devoted to investigate its mode of action along with its in vivo effectiveness and safety for clinical application. The anticancer activities of the molecules were also confirmed and detailed by molecular docking methods. The

results show that the silver complex could be a more effective anticancer agent than the ligand and this in silico result is in accordance with the experimental ones.

**Supplementary Materials:** The following supporting information can be downloaded at: <https://www.mdpi.com/article/10.3390/molecules27238131/s1>, FT-IR spectra of silver complexes **2** and **3**; X-ray structure of complexes **2** and **3**.

**Author Contributions:** Conceptualization, N.Ş., A.S. and D.S.; methodology, S.H., E.Ü., K.A.C. and Y.T.; software, E.Ü., K.A.C. and Y.T.; validation, N.Ş. and D.S.; formal analysis, N.Ş. and D.S.; investigation, S.H., E.Ü., K.A.C. and Y.T.; writing—original draft preparation, S.H., N.Ş. and D.S.; writing—review and editing, D.S.; supervision, D.S. All authors have read and agreed to the published version of the manuscript.

**Funding:** We gratefully acknowledge the Tunisian Ministry of Higher Education and Scientific Research for the financial support (grant for S.H.).

**Institutional Review Board Statement:** Not applicable.

**Informed Consent Statement:** Not applicable.

**Data Availability Statement:** The data presented in this study are available on request from the corresponding author.

**Conflicts of Interest:** The authors declare no conflict of interest.

**Sample Availability:** Samples of the compounds are not available from the authors.

## References

- Slenters, T.V.; Sague, J.L.; Brunetto, P.S.; Zuber, S.; Fleury, A.; Mirolo, L.; Robin, A.Y.; Meuwly, M.; Gordon, O.; Landmann, R.; et al. Of chains and rings: Synthetic strategies and theoretical investigations for tuning the structure of silver coordination compounds and their applications. *Materials* **2010**, *3*, 3407–3429. [CrossRef]
- Wang, X.-P.; Hu, T.-P.; Sun, D. Luminescent silver(I) coordination architectures containing 2-aminopyrimidyl ligands. *CrystEngComm* **2015**, *17*, 3393–3417. [CrossRef]
- Njogu, E.M.; Omondi, B.; Nyamori, V.O. Multimetallic silver(I)-pyridinyl complexes: Coordination of silver(I) and luminescence. *J. Coord. Chem.* **2015**, *68*, 3389–3431. [CrossRef]
- Balić, T.; Perdih, F.; Mršo, T.; Balić, I. Ligand influence on the formation of *exo*-coordinated silver(I) complexes with N<sub>2</sub>O<sub>2</sub> Schiff base macrocycles and the role of anion in supramolecular aggregation. *Polyhedron* **2020**, *190*, 114774. [CrossRef]
- Atif, M.; Bhatti, H.N.; Haque, R.A.; Iqbal, M.A.; Khadeer, M.B.A.; Majid, A.M.S.A. Synthesis, structure, and anticancer activity of symmetrical and non-symmetrical silver(I)-*N*-heterocyclic carbene complexes. *Appl. Biochem. Biotechnol.* **2020**, *191*, 1171–1189. [CrossRef]
- Şahin, N.; Şahin-Bölükbsi, S.; Tahir, M.N.; Arıcı, C.; Çevik, E.; Gürbüz, N.; Özdemir, İ.; Cummings, B.S. Synthesis, characterization and anticancer activity of allyl substituted *N*-heterocyclic carbene silver(I) complexes. *J. Mol. Struct.* **2019**, *1179*, 92–99. [CrossRef]
- Chiang, L.-M.; Yeh, C.-W.; Chan, Z.-K.; Wang, K.-M.; Chou, Y.-C.; Chen, J.-D.; Wang, J.-C.; Lai, J.Y. Ag(I) complexes containing *N*-phenyl-*N'*-cyano-formamidine: Syntheses, structures, and ligand conformations. *Cryst. Growth Des.* **2008**, *8*, 470–477. [CrossRef]
- Sandeli, A.E.-K.; Khiri-Meribout, N.; Benzerka, S.; Gürbüz, N.; Dünder, M.; Karci, H.; Bensouici, G.; Mokrani, E.L.; Özdemir, İ.; Koç, A.; et al. Silver(I)-*N*-heterocyclic carbene complexes: Synthesis and characterization, biological evaluation of anti-cholinesterase, anti-alpha-amylase, anti-lipase, and antibacterial activities, and molecular docking study. *Inorg. Chim. Acta* **2021**, *525*, 120486. [CrossRef]
- Wen, Q.-S.; Zhou, C.-L.; Qin, D.-Q. Acta diacetonitrile (3-[2-[8-(2-bromoethoxy)-9,10-dioxoanthracen-1-yloxy] ethyl]-1-(2-pyridylmethyl)imidazolium) silver(I) bis(hexafluoridophosphate). *Crystallogr. Sect. E* **2010**, *66*, m1030. [CrossRef]
- Chen, S.; Huang, Y.; Fang, X.; Li, H.; Zhang, Z.; Hor, T.S.A.; Weng, Z. Aryl-BIAN-ligated silver(i) trifluoromethoxide complex. *Dalton Trans.* **2015**, *44*, 19682–19686. [CrossRef]
- Osawa, M.; Hoshino, M. Brilliant reversible luminescent mechanochromism of silver(I) complexes containing *o*-bis(diphenylphosphino)benzene and phosphinesulfide. *Chem. Commun.* **2008**, *11*, 6384–6386. [CrossRef] [PubMed]
- Young, A.G.; Hanton, L.R. Square planar silver(I) complexes: A rare but increasingly observed stereochemistry for silver(I). *Coord. Chem. Rev.* **2008**, *252*, 1346–1386. [CrossRef]
- Nayeri, S.; Jamali, S.; Jamjah, A.; Shakirova, J.R.; Tunik, S.P.; Gurzhiy, V.; Samouei, H.; Shahsavari, H.R. Five- and six-coordinated silver(I) complexes formed by a metallomacrocyclic ligand with a “Au<sub>2</sub>N<sub>2</sub>” donor group: Observation of pendulum and linear motions and dual phosphorescence. *Inorg. Chem.* **2020**, *59*, 5702–5712. [CrossRef] [PubMed]
- Prince, P.D.; Steed, J. Weak interactions in silver complexes of 15-Crown-5. *Supramol. Chem.* **1998**, *10*, 155–158. [CrossRef]
- Jones, P.G.; Gries, T.; Grützmacher, H.; Roesky, H.W.; Schimkowiak, J.; Sheldrick, G.M. Silver-catalyzed formation of crown ethers; synthesis and structure of [Ag([12]crown-4)<sub>2</sub>][AsF<sub>6</sub>]. *Angew. Chem. Int. Ed.* **1984**, *23*, 376. [CrossRef]



16. Khlobystov, A.N.; Blake, A.J.; Champness, N.R.; Lemenovskii, D.A.; Majouga, A.G.; Zyk, N.V.; Schröder, M. Supramolecular design of one-dimensional coordination polymers based on silver(I) complexes of aromatic nitrogen-donor ligands. *Coord. Chem. Rev.* **2001**, *222*, 155–192. [[CrossRef](#)]
17. Zheng, S.-L.; Tong, M.-L.; Chen, X.-M. Silver(I)–hexamethylenetetramine molecular architectures: From self-assembly to designed assembly. *Coord. Chem. Rev.* **2003**, *246*, 185–202. [[CrossRef](#)]
18. Dong, Y.-B.; Wang, H.-Y.; Ma, J.-P.; Shen, D.-Z.; Huang, R.-Q. Synthesis and characterization of new coordination polymers generated from bent bis(cyanophenyl)oxadiazole ligands and Ag(I) salts. *Inorg. Chem.* **2005**, *44*, 4679–4692. [[CrossRef](#)]
19. Dong, Y.-B.; Cheng, J.-Y.; Ma, J.-P.; Huang, R.-Q. Self-assembly of  $\{Ag_2N_4\}$ -core-containing coordination polymers from AgX ( $X = NO_3^-$ ,  $ClO_4^-$ , and  $PF_6^-$ ) and oxadiazole-bridged 4,4'- and 3,3'-biphenylamine ligands. *Cryst. Growth Des.* **2005**, *5*, 585–591. [[CrossRef](#)]
20. Du, M.; Zhao, X.-J.; Guo, J.-H.; Batten, S.R. Direction of topological isomers of silver(I) coordination polymers induced by solvent, and selective anion-exchange of a class of PtS-type host frameworks. *Chem. Commun.* **2005**, *38*, 4836–4838. [[CrossRef](#)]
21. Dong, Y.-B.; Xu, H.-X.; Ma, J.-P.; Huang, R.-Q. Silver(I) coordination polymers based on a nano-sized bent bis(3-acetylenylphenyl-(4-cyanophenyl))oxadiazole ligand: The role of ligand isomerism and the templating effect of polyatomic anions and solvent intermediates. *Inorg. Chem.* **2006**, *45*, 3325–3343. [[CrossRef](#)] [[PubMed](#)]
22. Zhang, Q.; Ma, J.-P.; Wang, P.; Shi, Z.-Q.; Dong, Y.-B.; Huang, R.-Q. Unusual Ni–Ag mixed-metal, mixed-valence, and cluster-containing coordination polymers generated from nickel-macrocylic ligand and silver ion by metal-exchange. *Cryst. Growth Des.* **2008**, *8*, 2581–2587. [[CrossRef](#)]
23. Hou, G.-G.; Wu, Y.; Ma, J.-P.; Dong, Y.-B. Synthesis, structural characterization and properties of Ag(I)-complexes based on double-armed 1,3,4-oxadiazole bridging ligands. *CrystEngComm* **2011**, *13*, 6850–6863. [[CrossRef](#)]
24. Cao, S.; Pei, Z.; Xu, Y.; Zhang, R.; Pei, Y. Polytriazole bridged with 2,5-diphenyl-1,3,4-oxadiazole moieties: A highly sensitive and selective fluorescence chemosensor for  $Ag^+$ . *RSC Adv.* **2015**, *5*, 45888–45896. [[CrossRef](#)]
25. Dui, X.-J.; Wu, X.-Y.; Liao, J.-Z.; Teng, T.; Wu, W.-M.; Yang, W.-B. Photocatalytic properties of two POM-templated organic–inorganic hybrid compounds. *Inorg. Chem. Commun.* **2015**, *56*, 112–115. [[CrossRef](#)]
26. Ding, B.; Wu, J.; Wu, X.X.; Huo, J.Z.; Zhu, Z.Z.; Liu, Y.Y.; Shi, F.X. Syntheses, structural diversities and characterization of a series of coordination polymers with two isomeric oxadiazol-pyridine ligands. *RSC Adv.* **2017**, *7*, 9704–9718. [[CrossRef](#)]
27. Anghel, C.; Matache, M.; Paraschivescu, C.C.; Madalan, A.M.; Andruh, M. A novel 1-D coordination polymer constructed from disilver-1,3,4-oxadiazole nodes and perchlorato bridges. *Inorg. Chem. Commun.* **2017**, *76*, 22–25. [[CrossRef](#)]
28. Zheng, T.; Sun, A.; Guo, Y.; Bu, D.; Wang, Z.; Qu, Z. Synthesis and crystal structure of a novel polymeric silver(I) complex. *Mol. Cryst. Liq. Cryst.* **2018**, *666*, 94–99. [[CrossRef](#)]
29. Dong, Y.-B.; Ma, J.-P.; Huang, R.-Q.; Smith, M.D.; Loye, H.-C.Z. Synthesis and characterization of new coordination polymers generated from oxadiazole-containing organic ligands and inorganic silver(I) salts. *Inorg. Chem.* **2003**, *42*, 294–300. [[CrossRef](#)]
30. Dong, Y.-B.; Sun, T.; Ma, J.-P.; Zhao, X.-X.; Huang, R.-Q. Ag(I) and Cu(II) discrete and polymeric complexes based on single- and double-armed oxadiazole-bridging organic clips. *Inorg. Chem.* **2006**, *45*, 10613–10628. [[CrossRef](#)]
31. Zhao, L.; Xie, L.-Y.; Du, X.-L.; Zheng, K.; Xie, T.; Huang, R.-R.; Qin, J.; Ma, J.-P.; Ding, L.-H. Structural diversity in oxadiazole-containing silver complexes dependent on the anions. *Acta Chim. Slov.* **2020**, *67*, 822–829. [[CrossRef](#)] [[PubMed](#)]
32. Kokunov, Y.V.; Gorbunova, Y.E.; Popov, L.D.; Kovalev, V.V.; Razgonyaeva, G.A.; Kozyukhin, S.A.; Borodkin, S.A. Coordination silver polymer with the bridging anion of oxadiazolylacrylic acid: Synthesis, crystal structure, and luminescence properties. *Russ. J. Inorg. Chem.* **2016**, *42*, 361–366. [[CrossRef](#)]
33. Tan, S.J.; Yan, Y.K.; Lee, P.P.F.; Lim, K.H. Copper, gold and silver compounds as potential new anti-tumor metallodrugs. *Futur. Med. Chem.* **2010**, *2*, 1591–1608. [[CrossRef](#)] [[PubMed](#)]
34. Fromm, K.M. Silver coordination compounds with antimicrobial properties. *Appl. Organomet. Chem.* **2013**, *27*, 683–687. [[CrossRef](#)]
35. Banti, C.N.; Hadjikakou, S.K. Anti-proliferative and anti-tumor activity of silver(I) compounds. *Metallomics* **2013**, *5*, 569–596. [[CrossRef](#)]
36. Medici, S.; Peana, M.; Crisponi, G.; Nurchi, V.M.; Lachowicz, J.I.; Remelli, M.; Zoroddu, M.A. Silver coordination compounds: A new horizon in medicine. *Coord. Chem. Rev.* **2016**, *327*, 349–359. [[CrossRef](#)]
37. Rusu, A.; Hancu, G.; Munteanu, A.C.; Uivarosi, V. Development perspectives of silver complexes with antibacterial quinolones: Successful or not? *J. Organomet. Chem.* **2017**, *839*, 19–30. [[CrossRef](#)]
38. Liang, X.; Luan, S.; Yin, Z.; He, M.; He, C.; Yin, L.; Zou, Y.; Yuan, Z.; Li, L.; Song, X.; et al. Recent advances in the medical use of silver complex. *Eur. J. Med. Chem.* **2018**, *157*, 62–80. [[CrossRef](#)]
39. Hecel, A.; Kolkowska, P.; Krzywoszynska, K.; Szebesczyk, A.; Rowinska-Zyrek, M.; Kozlowski, H.  $Ag^+$  Complexes as Potential Therapeutic Agents in Medicine and Pharmacy. *Curr. Med. Chem.* **2019**, *26*, 624–647. [[CrossRef](#)]
40. Üstün, E.; Özdemir, N.; Şahin, N. Activity analysis of new *N*-heterocyclic carbenes and silver *N*-heterocyclic carbene molecules against novel coronavirus by UV-vis, fluorescence spectroscopy and molecular docking. *J. Coord. Chem.* **2021**, *74*, 3109–3126. [[CrossRef](#)]
41. Üstün, E.; Şahin, N.; Çelik, C.; Tutar, U.; Özdemir, N.; Gürbüz, N.; Özdemir, I. Synthesis, characterization, antimicrobial and antibiofilm activity, and molecular docking analysis of NHC precursors and their Ag–NHC complexes. *Dalton Trans.* **2021**, *50*, 15400–15412. [[CrossRef](#)] [[PubMed](#)]



42. Çevik-Yıldız, E.; Şahin, N.; Şahin-Bölükbaşı, S. Synthesis, characterization, and investigation of antiproliferative activity of novel Ag(I)-N-Heterocyclic carbene (NHC) compounds. *J. Mol. Struct.* **2020**, *1199*, 126987. [\[CrossRef\]](#)
43. Şahin-Bölükbaşı, S.; Cantürk-Kiliçkaya, P.; Kiliçkaya, O. Silver(I)-N-heterocyclic carbene complexes challenge cancer; evaluation of their anticancer properties and in silico studies. *Drug Dev. Res.* **2021**, *82*, 907–926. [\[CrossRef\]](#) [\[PubMed\]](#)
44. Akkoç, M.; Khan, S.; Yüce, H.; Türkmen, N.B.; Yaşar, Ş.; Yaşar, S.; Özdemir, I. Molecular docking and in vitro anticancer studies of silver(I)-N-heterocyclic carbene complexes. *Heliyon* **2022**, *8*, e10133. [\[CrossRef\]](#) [\[PubMed\]](#)
45. Hadrup, N.; Sharma, A.K.; Loeschner, K. Toxicity of silver ions, metallic silver, and silver nanoparticle materials after in vivo dermal and mucosal surface exposure: A review. *Regul. Toxicol. Pharmacol.* **2018**, *98*, 257–267. [\[CrossRef\]](#)
46. Dasari, S.; Tchounwou, P.B. Cisplatin in cancer therapy: Molecular mechanisms of action. *Eur. J. Pharmacol.* **2014**, *740*, 364–378. [\[CrossRef\]](#) [\[PubMed\]](#)
47. Zhou, J.; Kang, Y.; Chen, L.; Wang, H.; Liu, J.; Zeng, S.; Yu, L. The drug-resistance mechanisms of five platinum-based anti-tumor agents. *Front. Pharmacol.* **2020**, *11*, 343. [\[CrossRef\]](#)
48. Gacche, R.N. Compensatory angiogenesis and tumor refractoriness. *Oncogenesis* **2015**, *4*, e153. [\[CrossRef\]](#)
49. Kerbel, R.S. Tumor angiogenesis: Past, present and the near future. *Carcinogenesis* **2000**, *21*, 505–515. [\[CrossRef\]](#)
50. Ferrara, N. Vascular endothelial growth factor. *Arterioscler. Thromb. Vasc. Biol.* **2009**, *29*, 789–791. [\[CrossRef\]](#)
51. Kaipainen, A.; Korpelainen, E.; Alitalo, K. Vascular endothelial growth factor receptors. In *Tumor Angiogenesis and Microcirculation*; Voest, E.E., D'Amore, P.A., Eds.; Springer: New York, NY, USA, 2001; pp. 199–212.
52. Wang, X.; Bove, A.M.; Simone, G.; Ma, B. Molecular bases of VEGFR-2-mediated physiological function and pathological role front. *Cell Dev. Biol.* **2020**, *8*, 599281. [\[CrossRef\]](#)
53. Modi, S.J.; Kulkarni, V.M. Vascular Endothelial growth factor receptor (VEGFR-2)/KDR inhibitors: Medicinal chemistry perspective. *Med. Drug Discov.* **2019**, *2*, 100009. [\[CrossRef\]](#)
54. Glomb, T.; Szymankiewicz, K.; Świątek, P. Anti-cancer activity of derivatives of 1,3,4-oxadiazole. *Molecules* **2018**, *23*, 3361. [\[CrossRef\]](#) [\[PubMed\]](#)
55. Kafarski, P.; Lejczak, B. Biological activity of aminophosphonic acids. *Phosphorus Sulfur Silicon Relat. Elem.* **1991**, *63*, 193–215. [\[CrossRef\]](#)
56. Abdou, W.M.; Barghash, R.F.; Bekheit, M.S. Carbodiimides in the synthesis of enamino- and  $\alpha$ -aminophosphonates as peptidomimetics of analgesic/antiinflammatory and anticancer agents. *Arch. Pharm. Chem. Life Sci.* **2012**, *345*, 884–895. [\[CrossRef\]](#) [\[PubMed\]](#)
57. Bhattacharya, A.K.; Raut, D.S.; Rana, K.C.; Polanki, I.K.; Khan, M.S.; Iram, S. Diversity-oriented synthesis of  $\alpha$ -aminophosphonates: A new class of potential anticancer agents. *Eur. J. Med. Chem.* **2013**, *66*, 146–152. [\[CrossRef\]](#)
58. Yao, G.-Y.; Ye, M.-Y.; Huang, R.-Z.; Li, Y.-J.; Pan, Y.-M.; Xu, Q.; Liao, Z.-X.; Wang, H.-S. Synthesis and antitumor activities of novel rhein  $\alpha$ -aminophosphonates conjugates. *Bioorganic Med. Chem. Lett.* **2014**, *24*, 501–507. [\[CrossRef\]](#)
59. Cingolani, A.; Effendy; Martini, D.; Pettinari, C.; Skelton, B.W.; White, A.H. Synthesis, spectroscopic and structural characterization of novel adducts of some silver(I) salts with the ambidentate donor PPh<sub>2</sub>py. *Inorg. Chim. Acta* **2006**, *359*, 2183–2193. [\[CrossRef\]](#)
60. Bondi, A. Van der Waals Volumes and Radii. *J. Phys. Chem.* **1964**, *68*, 441–451. [\[CrossRef\]](#)
61. Schmidbaur, H.; Schier, A. Argentophilic interactions. *Angew. Chem. Int. Ed.* **2014**, *54*, 746–784. [\[CrossRef\]](#)
62. Fiore, C.; Sovic, I.; Lukin, S.; Halasz, I.; Martina, K.; Delogu, F.; Ricci, P.C.; Porcheddu, A.; Shemchuk, O.; Braga, D.; et al. Kabachnik–Fields reaction by mechanochemistry: New horizons from old methods. *ACS Sustain. Chem. Eng.* **2020**, *8*, 18889–18902. [\[CrossRef\]](#)
63. Hkiri, S. (5-Phényl-1,3,4-oxadiazol-2-yl)- $\alpha$ -aminophosphonates: Synthèse, Coordination et Applications Catalytiques. Ph.D. Thesis, Carthage University, Carthage, Tunisia, January 2022.
64. Suberu, J.O.; Romero-Canelón, I.; Sullivan, N.; Lapkin, A.A.; Barker, G.C. Comparative cytotoxicity of artemisinin and cisplatin and their interactions with chlorogenic acids in MCF7 breast cancer cells. *ChemMedChem* **2014**, *9*, 2791–2797. [\[CrossRef\]](#) [\[PubMed\]](#)
65. Tan, J.; Li, C.; Wang, Q.; Li, S.; Chen, S.; Zhang, J.; Wang, P.C.; Ren, L.; Liang, X.-J. A Carrier-free nanostructure based on platinum(IV) prodrug enhances cellular uptake and cytotoxicity. *Mol. Pharm.* **2018**, *15*, 1724–1728. [\[CrossRef\]](#) [\[PubMed\]](#)
66. Wang, C.-H.; Shih, W.-C.; Chang, H.C.; Kuo, Y.-Y.; Hung, W.-C.; Ong, T.-G.; Li, W.-S. Preparation and characterization of amino-linked heterocyclic carbene palladium, gold, and silver complexes and their use as anticancer agents that act by triggering apoptotic cell death. *J. Med. Chem.* **2011**, *54*, 5245–5249. [\[CrossRef\]](#) [\[PubMed\]](#)
67. Ferreira, E.; Munyaneza, A.; Omondi, B.; Meijboom, R.; Cronjé, M.J. The effect of 1:2 Ag(I) thiocyanate complexes in MCF-7 breast cancer cells. *BioMetals* **2015**, *28*, 765–781. [\[CrossRef\]](#)
68. Jaros, S.W.; Komarnicka, U.K.; Kyzioł, A.; Pucelik, B.; Nesterov, D.S.; Kirillov, A.M.; Smoleński, P. Therapeutic potential of a water-soluble silver-diclofenac coordination polymer on 3D pancreatic cancer spheroids. *J. Med. Chem.* **2022**, *65*, 11100–11110. [\[CrossRef\]](#)
69. Żyro, D.; Śliwińska, A.; Szymczak-Pajor, I.; Stręk, M.; Ochocki, J. Light Stability, Pro-apoptotic and genotoxic properties of silver(I) complexes of metronidazole and 4-hydroxymethylpyridine against pancreatic cancer cells in vitro. *Cancers* **2020**, *12*, 3848. [\[CrossRef\]](#)
70. Cozza, G.; Moro, S. Medicinal chemistry and the molecular operating environment (MOE): Application of QSAR and molecular docking to drug discovery. *Curr. Top. Med. Chem.* **2008**, *8*, 1555–1572. [\[CrossRef\]](#)

71. Ooms, F. Molecular modeling and computer aided drug design. Examples of their applications in medicinal chemistry. *Curr. Med. Chem.* **2000**, *7*, 141–158. [[CrossRef](#)]
72. Morris, G.M.; Lim-Wilby, M. Molecular docking. In *Molecular Modeling of Proteins*; Kukol, A., Ed.; Humana Press: Totowa, NJ, USA, 2008; pp. 365–382.
73. Boda, S.; Nukala, S.K.; Manchal, R. One-pot synthesis of some new isatin-1,2,4-oxadiazole hybrids as VEGFR-2 aiming anticancer agents. *ChemistrySelect* **2022**, *7*, e202200972. [[CrossRef](#)]
74. Serdaroglu, G.; Şahin, N.; Şahin-Bölükbaşı, S.; Üstün, E. Novel Ag(I)-NHC complex: Synthesis, in vitro cytotoxic activity, molecular docking, and quantum chemical studies. *Z. Naturforsch. C J. Biosci.* **2021**, *77*, 21–36. [[CrossRef](#)] [[PubMed](#)]
75. Ali, O.M.; Alotaibi, M.T.; Zaki, Y.H.; Amer, H.H. Design, synthesis, and spectroscopic studies of some new  $\alpha$ -aminophosphonate analogues derived from 4-hydroxybenzaldehyde with special reference to anticancer activity. *Drug Des. Dev. Ther.* **2022**, *16*, 2589–2599. [[CrossRef](#)] [[PubMed](#)]
76. Oubella, A.; El Mansouri, A.-E.; Fawzi, M.; Bimoussa, A.; Laamari, Y.; Auhmani, A.; Morjani, H.; Robert, A.; Riahi, A.; Itto, M.Y.A. Thiazolidinone-linked 1,2,3-triazoles with monoterpene skeleton as new potential anticancer agents: Design, synthesis and molecular docking studies. *Bioorganic Chem.* **2021**, *115*, 105184. [[CrossRef](#)]
77. Zhang, B.; Hu, X.-T.; Gu, J.; Yang, Y.-S.; Duan, Y.-T.; Zhu, H.-L. Discovery of novel sulfonamide-containing aminophosphonate derivatives as selective COX-2 inhibitors and anti-tumor candidates. *Bioorganic Chem.* **2020**, *105*, 104390. [[CrossRef](#)] [[PubMed](#)]
78. Amer, H.H.; Alotaibi, S.H.; Trawneh, A.H.; Metwaly, A.M.; Eissa, I.H. Anticancer activity, spectroscopic and molecular docking of some new synthesized sugar hydrazones, arylidene and  $\alpha$ -aminophosphonate derivatives. *Arab. J. Chem.* **2021**, *14*, 103348. [[CrossRef](#)]
79. Khidre, M.; Abdelaleem, F.; Abu Bakr, S.; Awad, H.; Sabry, E. Novel synthesis, docking studies and antitumor evaluation of pyrazolo- and pyrazolo aminophosphonate derivatives derived from *N*-heterocyclic amines. *Egypt. J. Chem.* **2022**, *65*, 657–672. [[CrossRef](#)]
80. Neese, F. The ORCA program system. *WIREs Comput. Mol. Sci.* **2012**, *2*, 73–78. [[CrossRef](#)]
81. Neese, F.; Wennmohs, F.; Becker, U.; Riplinger, C. The ORCA quantum chemistry program package. *J. Chem. Phys.* **2020**, *152*, 224108. [[CrossRef](#)]
82. Miyazaki, Y.; Matsunaga, S.; Tang, J.; Maeda, Y.; Nakano, M.; Philippe, R.J.; Shibahara, M.; Liu, W.; Sato, H.; Wang, L.; et al. Novel 4-amino-furo[2,3-d]pyrimidines as Tie-2 and VEGFR2 dual inhibitors. *Bioorganic Med. Chem. Lett.* **2005**, *15*, 2203–2207. [[CrossRef](#)]
83. Gupta, R.K.; Sharma, G.; Pandey, R.; Kumar, A.; Koch, B.; Li, P.-Z.; Xu, Q.; Pandey, D.S. DNA/Protein binding, molecular docking, and in vitro anticancer activity of some thioether-dipyrrinato complexes. *Inorg. Chem.* **2013**, *52*, 13984–13996. [[CrossRef](#)]
84. Drew, H.R.; Wing, R.M.; Takano, T.; Broka, C.; Tanaka, S.; Itakura, K.; Dickerson, R.E. Structure of a B-DNA dodecamer: Conformation and dynamics. *Proc. Natl. Acad. Sci. USA* **1981**, *78*, 2179–2183. [[CrossRef](#)] [[PubMed](#)]
85. Hkiri, S.; Gourlaouen, C.; Touil, S.; Samarat, A.; Sémeril, D. 1,3,4-Oxadiazole-functionalized  $\alpha$ -amino-phosphonates as ligands for the ruthenium-catalyzed reduction of ketones. *New J. Chem.* **2021**, *45*, 11327–11335. [[CrossRef](#)]
86. Sheldrick, G.M. SHELXT—Integrated space-group and crystal-structure determination. *Acta Crystallogr. Sect. A* **2015**, *71*, 3–8. [[CrossRef](#)] [[PubMed](#)]
87. Sheldrick, G.M. A short history of SHELX. *Acta Crystallogr. Sect. A* **2008**, *A64*, 112–122. [[CrossRef](#)] [[PubMed](#)]
88. Sheldrick, G.M. Crystal structure refinement with SHELXL. *Acta Crystallogr. Sect. C* **2015**, *C71*, 3–8. [[CrossRef](#)]
89. Mosmann, T. Rapid colorimetric assay for cellular growth and survival: Application to proliferation and cytotoxicity assays. *J. Immunol. Methods* **1983**, *65*, 55–63. [[CrossRef](#)]
90. Morris, G.M.; Huey, R.; Lindstrom, W.; Sanner, M.F.; Belew, R.K.; Goodsell, D.S.; Olson, A.J. AutoDock4 and AutoDockTools4: Automated docking with selective receptor flexibility. *J. Comput. Chem.* **2009**, *30*, 2785–2791. [[CrossRef](#)]
91. Morris, G.M.; Goodsell, D.S.; Halliday, R.S.; Huey, R.; Hart, W.E.; Belew, R.K.; Olson, A.J. Automated docking using a Lamarckian genetic algorithm and an empirical binding free energy function. *J. Comp. Chem.* **1998**, *19*, 1639–1662. [[CrossRef](#)]